Acta Oceanol. Sin., 2024, Vol. 43, No. 10, P. 86–99
https://doi.org/10.1007/s13131-024-2385-9
http://www.aosocean.com
E-mail: ocean2@hyxb.org.cn

Major ions and trace metals in glacial meltwaters nearby Ny-Ålesund, Svalbard

Zhan Shen[1†], Liping Ye[2†], Jing Zhang[1, 2], Hongmei Ma[3], Ruifeng Zhang[1, 2, 3, 4*]

[1] Key Laboratory of Polar Ecosystem and Climate Change of Ministry of Education and School of Oceanography, Shanghai Jiao Tong University, Shanghai 200030, China

[2] State Key Laboratory of Estuarine and Coastal Research, East China Normal University, Shanghai 200062, China

[3] Laboratory for Polar Science, Polar Research Institute of China, Ministry of Natural Resources, Shanghai 200136, China

[4] Shanghai Key Laboratory of Polar Life and Environment Sciences, Shanghai Jiao Tong University, Shanghai 200030, China

Received 19 March 2024; accepted 31 May 2024

Abstract

Ny-Ålesund, located in Arctic Svalbard, is one of the most sensitive areas on Earth to global warming. In recent years, accelerated glacier ablation has become remarkable in Ny-Ålesund. Glacial meltwaters discharge a substantial quantity of materials to the ocean, affecting downstream ecosystems and adjacent oceans. In August 2015, various water samples were taken near Ny-Ålesund, including ice marginal meltwater, proglacial meltwater, supraglacial meltwater, englacial meltwater, and groundwater. Trace metals (Al, Cr, Mn, Fe, Co, Cu, Zn, Cd, and Pb), major ions, alkalinity, pH, dissolved oxygen, water temperature and electric conductivity were also measured. Major ions were mainly controlled by chemical weathering intensity and reaction types, while trace metals were influenced by both chemical weathering and physicochemical control upon their mobility. Indeed, we found that Brøggerbreen was dominated by carbonate weathering via carbonation of carbonate, while Austre Lovénbreen and Pedersenbreen were dominated by sulfide oxidation coupled with carbonate dissolution with a doubled silicate weathering. The higher enrichment of trace metals in supraglacial meltwater compared to ice marginal and proglacial meltwater suggested anthropogenic pollution from atmospheric deposition. In ice marginal and proglacial meltwater, principal component analysis indicated that trace metals like Cr, Al, Co, Mn and Cd were correlated to chemical weathering. This implies that under accelerated glacier retreat, glacier-derived chemical components are subjected to future changes in weathering types and intensity.

Key words: Arctic, glacial meltwater, weathering, major ions, trace metals

Citation: Shen Zhan, Ye Liping, Zhang Jing, Ma Hongmei, Zhang Ruifeng. 2024. Major ions and trace metals in glacial meltwaters nearby Ny-Ålesund, Svalbard. Acta Oceanologica Sinica, 43(10): 86–99, doi: 10.1007/s13131-024-2385-9

1 Introduction

Glaciers contain about 70% of the global fresh water resources on earth. Polar regions are some of the most sensitive regions with respect to climate changes. According to the IPCC (2019) reports, almost all glaciers are experiencing continuous retreat, especially in the Arctic and the west Antarctica regions (Hugonnet et al., 2021). For quite some time, polar regions were considered too remote for direct, noticeable effects of anthropogenic activities, but activities such as tourism, mining, shipping, and long-range atmospheric transport are increasingly having an impact (Vargo et al., 2020). Therefore, the polar regions are suffering from not only a warming climate, but also from environmental and ecological issues. The feedbacks to these environmental and anthropogenic driving forces therefore draw lots of attention to the polar regions.

Hydrochemical parameters, such as major ions and alkalinity, are usually studied to understand aqueous weathering and environmental conditions (Nowak and Hodson, 2014; Yde et al., 2014). They help researchers comprehend the weathering and environmental processes in glacierized catchments that respond to changing climate (Graly et al., 2014; Ingri et al., 2005). As melting accelerates, glacial meltwater carries large freshwater and material fluxes into the adjacent ocean (Nowak and Hodson, 2013), making it urgent to study their environmental and ecological consequences. Among these fluxes, trace metals have attracted attention due to their distinctive roles in tracing geochemical and environmental processes, as well as fertilizing or poisoning marine biota (Morel and Price, 2003). For example, Al and Mn are usually applied as tracers to reveal the lithogenic sources or redox processes (Ren et al., 2006), while Fe, Co, Zn and Mn are essential elements for marine phytoplankton that regulate primary production in some ocean regions (Gerringa et al., 2020; Tagliabue et al., 2017; Vance et al., 2017; Huertas et al., 2014). Cd and Cu act as either stimulating or toxic elements to marine life,

Foundation item: The National Natural Science Foundation of China under contract Nos 42076227, 41676175 and 41276202; the Chinese Arctic and Antarctic Administration under contract No. CHINARE-YRS2015–21; the Shanghai Pilot Program for Basic Research—Shanghai Jiao Tong University under contract No. 21TQ1400201; the Shanghai Frontiers Science Center of Polar Science (SCOPS).

*Corresponding author, E-mail: ruifengzhang@sjtu.edu.cn

†These authors contributed equally to this work.

depending on their concentration levels (Miao et al., 2005), while Cr and Pb are harmful elements for health that create environmental issues (Pratush et al., 2018).

Ny-Ålesund is located on Svalbard, where the Arctic Ocean and Atlantic Ocean connect. The Ny-Ålesund area is characterized as subarctic with respect to climate, and has a landscape consisting of fjords, glaciers, meltwater, and tundra (Willis et al., 2006). Fresh water in Ny-Ålesund mainly comes from glacier melting, snow and ice melting, and summer precipitation, and the melting season is typically from late April to September (Nowak and Hodson, 2014; Svendsen et al., 2002). The bedrocks are mainly Carboniferous-Permian limestone and dolomite to the west, and older metamorphic phyllite and schists to the east, especially beneath the glaciers' accumulation areas (Dallmann, 2015). Ny-Ålesund is also subjected to a warming climate, such that data from the environmental monitoring of Svalbard and Jan Mayen (MOSJ) shows the mass balance in Austre Brøggerbreen glacier and Midtre Lovénbreen glacier was almost always negative from 1968 to 2018 (http://www.mosj.no/en/climate/). During the past 50 years, the thickness of the two glaciers has decreased by 23.4 m and 18.2 m, respectively. Previous studies have suggested that the hydrochemistry in Bayelva River is controlled both by snowpack solute elution and chemical weathering (Nowak and Hodson, 2015; Hodson et al., 2002, 2000). At Austre Brøggerbreen, chemical weathering in Bayelva River is dominated by calcite at high elevations, while downstream weathering in the proglacial environment is dominated by a combination of calcite and dolomite dissolution weathering which doubled the Mg^{2+}, Ca^{2+} and HCO_3^- concentrations along the flow path (Hodson et al., 2002). The same work shows that concentrations of SO_4^{2-} also increase downstream because sulfide oxidation is an important source of acidity for weathering reactions in the glacier forefield and moraines. A 20-year period of observations from the Bayelva River suggested that chemical weathering was enhanced by the increased exposure of the proglacial area following the retreat of Austre Brøggerbreen. No delayed subglacial drainage pathways exist beneath this glacier on account of its switch to a cold-based thermal regime following sustained mass balance losses (Nowak and Hodson, 2014, 2013). This transition greatly restricts the penetration of surface meltwaters to the glacier bed, and so the expanding glacier forefield became increasingly important for promoting extended rock-water contact as the cold-based glacier retreated. By contrast, at Midtre Lovénbreen, the chemical weathering processes are less affected by carbonate lithologies, and subglacial weathering processes are more important, especially with respect to sulfide oxidation and its effect upon carbonate weathering (Irvine-Fynn and Hodson, 2010; Hodson et al., 2000).

Trace metals in meltwater originate predominantly from both natural and anthropogenic processes, such as weathering, dissolution of local geological substratum, and atmospheric depositions. A few studies have addressed the soils in Ny-Ålesund (Rajaram et al., 2023; Halbach et al., 2017), the metals composition of aerosols from long-distance anthropogenic-derived transportation (Platt et al., 2022; Moroni et al., 2016) or summertime cruise ship emissions (Zhan et al., 2014). Zhang et al. (2015) applied iron isotopes to reveal that the aggregation and adsorption of nanoparticulate and colloidal Fe to particles were responsible for Fe loss in the proglacial environment within the Bayelva catchment. However, since most meltwater hydrology studies focus on Bayelva, there is a lack of studies on the processes that determine trace metals in meltwaters elsewhere in the region. A comprehensive study of major ions and trace metals in meltwaters from different meltwater systems near Ny-Ålesund is therefore necessary to understand natural and anthropogenic biogeochemical conditions in this important research environment.

In August 2015, five types of water samples including supraglacial meltwater, englacial meltwater, ice marginal meltwater, proglacial meltwater and groundwater, were sampled from four glacier systems near Ny-Ålesund. Major ions (Ca^{2+}, Mg^{2+}, Na^+, K^+, Cl^-, SO_4^{2-}), alkalinity, nutrients (NO_3^-, Si), and trace metals (Al, Cr, Mn, Fe, Co, Cu, Zn, Cd, and Pb) were measured. The aim of this study is to compare and complement the existing hydrology data for a better understanding of biogeochemical cycling in glacier systems, and to investigate baseline for trace metals and the potential anthropogenic fingerprint in Ny-Ålesund.

2 Method and study area

2.1 *Sampling and handling*

The area of sampling and sampled sites is shown in Fig. 1. The Svalbard archipelago (74°–81°N, 10°–35°E) consist of many islands, including Spitsbergen, Nordaustlandet, Barents Island, and others. It is located between the Barents Sea and the Greenland Sea, which are the channels of water exchange between the Arctic Ocean and the Atlantic Ocean (Hop et al., 2006; Svendsen et al., 2002). About 60% of the land in the Svalbard Archipelago is covered by glaciers, with estimated fluxes of meltwater and iceberg calving of (25 ± 5) km^3 and (4 ± 1) km^3 annually, respectively (Hagen et al., 2003). Ny-Ålesund is located in south of Kongsfjorden. There are five main glaciers around Ny-Ålesund on the south shore side of Kongsfjorden, including Vestre Brøggerbreen, Austre Brøggerbreen, Midtre Lovénbreen, Austre Lovénbreen, and Pedersenbreen. The main channel of Bayelva River derives from Austre Brøggerbreen, and it mixes with meltwater from Vestre Brøggerbreen in the middle-reach. Both Austre and Vestre Brøggerbreen are almost entirely cold-based. By contrast, Midtre Lovénbreen and Pedersenbreen offer extended opportunities for rock-water contact at the glacier bed due to the presence of temperate, subglacial ice (Irvine-Fynn et al., 2010). Lastly, little or nothing is known of the drainage system of Vestre Lovénbreen, although it has been suggested that it has also become cold-based according to research into a historic groundwater system thought to have been recharged by temperate ice in the accumulation area when the glacier was substantially thicker (Haldorsen et al., 2011).

Glacial meltwater sampling from four glaciers was carried out in August 2015, shown as in Fig. 1. Meltwater from Vestre Brøggerbreen as VB_{BOM}, Austre Brøggerbreen as AB_{UP}, AB_{MD}, and AB_{DW}, were taken twice for observing daily variation. Meltwater from Austre Lovénbreen as AL1–AL5, and Pedersenbreen as P1 and P2, were taken once. The sampling site for AB_{DW} was located at the Norwegian Water Resources and Energy Directorate (NVE) station, which is situated 2 km northwest of Ny-Ålesund and 300 m from the outlet of the Bayelva River into Kongsfjorden. A third sampling survey was also conducted at the AB_{DW} site. Additionally, one groundwater sample, namely GW, was collected from moss land in the Bayelva River basin. A total of 17 water samples were taken from five types of water sources: supraglacial meltwater flowing on the surface of Austre Lovénbreen (AL1, n = 1), englacial meltwater which is clear outflow water from an opening from Austre Lovénbreen (AL3, n = 1), groundwater near the Bayelva River (GW, n = 1), ice marginal meltwater (AB_{UP}, AL2, P1, n = 4), and proglacial meltwaters with high turbidity, derived from meltwater contacting the bedrock of each glacier (VB_{BOM}, AB_{MD}, AB_{DW}, AL4, AL5, and P2, n = 10).

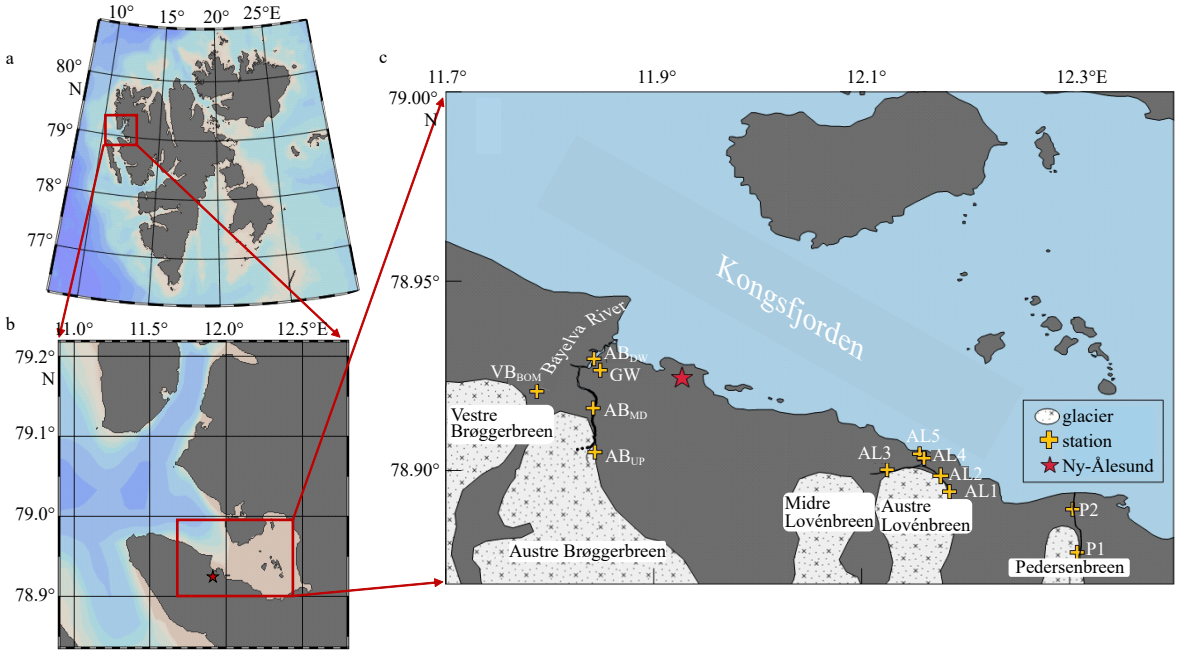

Fig. 1. Sample sites. a. Location of Ny-Ålesund on Svalbard Archipelago; b. map of Ny-Ålesund and Kongsfjorden; c. sampling sites in Ny-Ålesund in 2015.

At a riverbed approximately 200 m from ABDW station, a well with dimension of 1.5 m × 1.5 m × 1 m (width × length × depth) was dug, and the active-layer groundwater sample (GW) was taken after removing the overflow water three times. The GW station is characterized as a tundra ecosystem with permafrost. The continuous permafrost underlies the unglaciated area is around 100 m thick, and at the end of summer, the active layer ranges from 1 m to 2 m in thickness (Boike et al., 2018). Meltwater samples were collected using a custom-made "pole sampler", as described previously in Zhang et al. (2015). Briefly, a pre-cleaned 1 L high density polyethene (HDPE) bottle was attached to the top of the pole sampler, rinsed several times with meltwater from the middle of the main stream, then bottled with meltwater, sealed in double plastic bags, and kept in a cool box after sampling. Samples were taken on foot from upper stream to downstream, and then transported back to the marine lab onshore by rubber boat. Samples were filtered in class 100 clean flow bench in the marine lab immediately upon arrival using acid-cleaned 0.4 μm polycarbonate membrane (Whatman). Filtered samples for trace metal analysis were acidified to pH = 2 using ultrapure HCl, and kept in triple bags at room temperature until analysis. All plastic labware were pre-cleaned according to the protocol described in Zhang et al. (2015). Specificly, the plastic labwares were cleaned using the following procedures: soaking in 2% Citranox detergent overnight, followed by cleaning with ultra-pure water (Milli-Q) seven times. Next, they were soaked in 10% HCl for a week, then cleaned again with ultra-pure water seven times. Finally, they were packed in triple plastic bags. Auxiliary parameters, including temperature (T), pH, dissolved oxygen (DO), and electronic conductivity (EC), were collected on-site using a multi-parameter probe (WTW Multi 350i).

2.2 *Sample analysis*

2.2.1 *Hydrochemical parameters*

Major ions (including: Na^+, K^+, Mg^{2+}, Ca^{2+}, Cl^-, SO_4^{2-}) were measured using an Ion Chromatograph (Dionex, ICS-2000) at East China Normal University. The relative standard deviations for measuring the quality control standards of ions were less than 3%. Specifically, the total cationic equivalents (TC) were calculated as $[Na^+] + [K^+] + 2[Mg^{2+}] + 2[Ca^{2+}]$, while the total anion equivalents (TA) were calculated as $[Cl^-] + 2[SO_4^{2-}] + [HCO_3^-] + 2[CO_3^{2-}] + [NO_3^-]$. For all analyzed samples, the difference between TC and TA (|TC – TA|) was less than 0.02 meq/L (milligram equivalent), and the percentage difference (|TC – TA|/|TC + TA| × 100%) was less than 2%, verifying the quality of the measurement.

Alkalinity (Alk) was determined and calculated from the pH probe measurements, as described by Ye et al. (2018). The relative standard deviation (RSD) of measurements was less than 1.3%. Based on the total amount of HCl standard added and the remaining amount, we calculated alkalinity using following equation:

$$\mathrm{Alk} = [C_{\mathrm{HCl}} \times V_{\mathrm{T}} - 10^{(-\mathrm{pH})} \times (V_{\mathrm{T}} + V_{\mathrm{S}})]/V_{\mathrm{S}}, \quad (1)$$

where C_{HCl}, V_{T}, and V_{S} represent the concentration of standards HCl, total volume of HCl added, and the sample volume, respectively. We determined 3 measurements for each sample, and the difference between parallel samples was less than 0.02 pH unit.

$[HCO_3^-]$ was calculated using Eqs (2) and (3), which take into account the water temperature during measurement, as well as the water temperature and pH measured on-site by the WTW Multi 350i multi-parameter probe:

$$\mathrm{pH} < 8: [HCO_3^-] = \mathrm{Alk} - [OH^-] + [H^+] = \mathrm{Alk} - k_{\mathrm{w}} \times 10^{\mathrm{pH}} + 10^{-\mathrm{pH}}, \quad (2)$$

$$\mathrm{pH} \geqslant 8: [HCO_3^-] = \mathrm{Alk} - [OH^-] + [H^+]/(1 + 2 \times K_2/[H^+]), \quad (3)$$

where, k_{w} refers to the ionic product constant of water, and the

constant values under different temperatures were obtained from Perlt et al. (2017). k_2 refers to the dissociation constants of carbonic acid, which is calculated according to the method described by Millero et al. (2006) and Woosley and Moon (2023).

The concentrations of nutrients (NO_3^- and Si) were determined by colorimetry method using a continuous flow analyzer (SAN SKALAR Plus) at East China Normal University. The detection limits of NO_3^- and Si were 0.002 mg/L and 0.005 mg/L, respectively, and the relative standard deviations were 3% and 1%, respectively.

2.2.2 *Trace metals*

Trace metals (Al, Cr, Mn, Fe, Co, Cu, Zn, Cd, and Pb) were measured using a high resolution inductively coupled plasma mass spectrometer (Element 2, Thermo Fisher) at the University of Southern California. All samples were matched into a 0.1 mol/L HNO_3 matrix and determined by an external standard curve with 1 mg/L In as an internal standard. The detection limits for Al, Cr, Mn, Fe, Co, Cu, Zn, Cd, and Pb were 0.27 ng/L, 0.03 ng/L, 0.02 ng/L, 0.10 ng/L, 0.01 ng/L, 0.02 ng/L, 0.06 ng/L, 0.06 ng/L and 0.01 ng/L, respectively, with analytical precision <3%.

2.3 *Data process*

2.3.1 *Sea-salt correction*

Sea-salts can significantly influence some of the chemical components in Bayelva (Hodson et al., 2002), especially major ions. Thus, it is necessary to eliminate the contribution of sea-salt using Cl as a reference element (Grosbois et al., 2000), following equation:

$$^{*}[\mathrm{M}] = [\mathrm{M}]_{\mathrm{measure}} - \frac{[\mathrm{M}]_{\mathrm{sea}}}{[\mathrm{Cl}^-]_{\mathrm{sea}}} \times [\mathrm{Cl}^-]_{\mathrm{measure}}, \quad (4)$$

where, *[M] represents the concentration of major ions after sea-salt correction; $[\mathrm{M}]_{\mathrm{measure}}$ and $[\mathrm{Cl}^-]_{\mathrm{measure}}$ represent the measured values of major ion and Cl^- in samples, respectively; $[\mathrm{M}]_{\mathrm{sea}}/[\mathrm{Cl}^-]_{\mathrm{sea}}$ represents the ratio of major ion to Cl^- in seawater. The ratios for Na^+, K^+, Mg^{2+}, Ca^{2+}, and SO_4^{2-} to Cl^- are 0.86, 0.02, 0.097, 0.02, and 0.052, respectively.

2.3.2 *Statistical analysis*

Significance test (*t*-test), Principal Component Analysis (PCA) and Cluster Analysis (CA) were all completed using Statistical Package of the Social Sciences (SPSS, version 20.0). In the *t*-test, a result with *t* less than 0.05 is considered to indicate a significant difference. PCA analysis was employed to identify the primary controlling factors of trace metals among ice marginal and proglacial meltwater samples, while CA analysis was applied to identify the similarity of trace metal in ice marginal and proglacial meltwater. For PCA, the Kaiser-Meyer-Olkin (KMO) test and Bartlett's test of sphericity were used, and the maximum variance method was selected. A result of less than 0.001 for the sphericity test indicates correlation among the data and suggests further analysis can be done. Ward's method was chosen for cluster analysis, and Squared Euclidean distance was used as the measurement distance.

3 Results

3.1 *Major ions*

The average and range of major ions in all ice marginal and proglacial meltwater samples are shown in Table 1. Hydrochemistry parameter for all meltwater samples are shown in Table 2. The range of electronic conductivity (EC) was between 12 μS/cm and 110 μS/cm, with an average of (64 ± 39) μS/cm (n = 16). EC in the Bayelva River increased downstream, from an average of 34.5 μS/cm at Station AB_{UP} to an average value of 65.7 μS/cm at Station AB_{DW} before entering the sea. Temperature ranged from 0.5℃ to 5.9℃ and averaged (2.0 ± 1.5)℃ (n = 16). pH ranged from 7.59 to 9.10, averaging 8.43 ± 0.36 (n = 16); dissolved oxygen (DO) ranged from 10.2 mg/L to 14.4 mg/L with an average value of (12.6 ± 1.4) mg/L (n = 16). The main components of major ions in meltwater were Ca^{2+} for cations, and HCO_3^- and SO_4^{2-} for anions, respectively. Major ions concentration (μmol/L) followed the order of $[HCO_3^-] > [Ca^{2+}] > [SO_4^{2-}] > [Mg^{2+}] > [Cl^-] > [Na^+] > [K^+]$. The range of total cations (TC) was from 0.09 meq/L to 1.05 meq/L, while total anions (TA) was from 0.08 meq/L to 1.06 meq/L.

The groundwater at Site GW had the highest EC value and highest major ion concentrations among all water samples, while the lowest dissolved oxygen concentration was observed at this site with the value of 9.0 mg/L. Compared to the visible redness color in Bayelva River, meltwater from Vestre Brøggerbreen showed a greyish color and higher EC value. The highest HCO_3^- concentration with an average value of 46.70 mg/L, accompanying the highest alkalinity and pH values, were observed in meltwater from Vestre Brøggerbreen among the investigated meltwater samples. Samples from Sites AL1 and AL3 were supraglacial and englacial meltwater, respectively. Major ion and EC values at these two sites were lowest among the all types of waters. Among the ice marginal and proglacial meltwater, EC values ranked in the order of Austre Lovénbreen > Vestre Brøggerbreen ⩾ Pedersenbreen > Austre Brøggerbreen. The lowest Ca^{2+} value was observed in Austre Brøggerbreen, while highest SO_4^{2-} value was observed in Austre Lovénbreen.

3.2 *Trace metals*

Trace metal concentrations are shown in Table 3. In glacial meltwaters, the average concentrations of trace metals followed the order of Al > Mn > Fe > Cu > Co > Zn > Cr > Pb > Cd. The concentrations of Al and Mn in glacial meltwater near the ice margin ranged from 5.78 μg/L to 112.7 μg/L and from 0.99 μg/L to 40.42 μg/L, respectively. Fe in turbid glacial meltwater ranged from 0.22 μg/L to 8.39 μg/L, with the exception of a single maximum value of 116.8 μg/L at sampling site AL2. The detectable concentrations of Zn, Cu, Co, Cr, Pb, and Cd in ice marginal and proglacial meltwater ranged from 0 to 0.23 μg/L, 30.09 ng/L to

Table 1. Concentration range of major ions in ice marginal and proglacial meltwater in Ny-Ålesund (μmol/L, n = 14)

	Na^+	K^+	Mg^{2+}	Ca^{2+}	Cl^-	SO_4^{2-}	HCO_3^-	Si	NO_3^-
Average value	46.4	15.0	70.0	267	43.9	90.8	501	5.44	1.29
Standard deviation	15.4	7.9	24.9	72.5	18.5	77.1	147	2.56	0.67
Max value	76.1	29.4	119	358	84.6	245	773	9.86	2.58
Min value	27.8	7.2	23.4	126	20.3	21.9	305	2.23	0.32

Table 2. Summary table for electronic conductivity (EC, μS/cm), temperature (T, ℃), pH, dissolved oxygen (DO, mg/L), alkalinity (Alk, μmol/L), major ions (Na^+, K^+, Mg^{2+}, Ca^{2+}, Cl^-, SO_4^{2-}, HCO_3^- concentrations; μmol/L), nutrients (NO_3^-, Si concentrations; μmol/L), total cation and total anion (TC and TA milligram equivalent, meq/L), sulfate mass fraction (SMF) value, percentages (%) of four types solutes provenances including atmosphere (A), aerosol (E), marine (M) and crustal (U) sources

Water types	Source glacier	Station	EC	T	pH	DO	Alk	Na^+	K^+	Mg^{2+}	Ca^{2+}	Cl^-	SO_4^{2-}	HCO_3^-	Si	NO_3^-	$^*Na^+$	$^*K^+$	$^*Mg^{2+}$	$^*Ca^{2+}$	$^*SO_4^{2-}$	TC	TA	SMF	A	E	M	U
Ice marginal and proglacial meltwater (n = 14)	Austre Brøggerbreen	AB_{UP} (n = 2)	34	0.7	8.27	14.1	0.31	36.1	7.2	23.4	126	41.5	21.9	305	2.37	0.65	0.4	6.4	23.4	125	19.7	0.34	0.40	0.11	25	0	14	60
			35	0.8	8.35	13.8	0.33	37.8	8.7	37.4	158	41.2	26.2	325	2.23	1.77	2.2	7.9	37.4	157	24.0	0.44	0.43	0.13	24	0	13	63
		AB_{MD} (n = 2)	67	n.a.	8.21	13.3	0.49	44.8	12.8	77.3	227	54.2	76.7	487	4.47	1.13	n.a.	11.8	77.3	226	73.9	0.67	0.70	0.23	17	0	11	72
			46	1.1	8.05	14.4	0.42	46.1	10.7	42.0	200	41.5	34.5	418	2.5	1.61	10.4	10.0	42.0	199	32.4	0.54	0.53	0.13	26	0	10	63
		AB_{DW} (n = 3)	68	4.1	8.60	n.a.	0.63	35.2	9.7	72.0	269	29.9	41.9	619	5.26	0.48	9.6	9.2	72.0	268	40.4	0.73	0.74	0.12	28	0	5	67
			66	5.9	8.39	11.1	0.58	32.2	10.2	68.3	260	27.4	45.6	567	3.81	0.32	8.7	9.7	68.3	260	44.1	0.70	0.69	0.13	27	0	5	68
			63	2.3	8.26	13.2	0.59	40.0	13.3	63.3	267	31.3	44.8	583	3.29	1.45	13.0	12.5	63.3	266	43.1	0.71	0.71	0.13	28	0	6	66
	Vestre Brøggerbreen	AB_{BOM} (n = 2)	79	2.3	8.85	13.5	0.79	33.9	7.9	92.6	322	31.6	30.2	758	5.91	0.81	6.5	7.4	92.6	321	28.6	0.87	0.86	0.07	29	0	5	66
			85	2.3	8.45	13.0	0.78	27.8	8.4	93.4	331	20.3	40.1	773	4.99	1.77	10.4	7.9	93.4	330	39.0	0.88	0.89	0.09	29	0	3	68
	Austre Lovénbreen	AL2	110	0.5	8.13	10.3	0.55	76.1	29.4	119	355	84.6	203	549	9.86	1.94	3.5	27.9	119	354	199	1.05	1.06	0.42	9	0	11	79
		AL4	93	2.6	8.70	12.7	0.46	45.2	18.4	76.5	350	36.4	205	445	7.62	0.81	13.9	17.9	76.5	349	203	0.92	0.91	0.48	9	0	6	85
		AL5	103	3.4	7.69	10.8	0.41	62.6	18.9	87.6	358	47.4	245	409	6.97	0.81	21.7	18.2	87.6	358	242	0.97	0.96	0.54	11	0	7	81
	Pedersenbreen	P1	81	0.6	8.60	10.2	0.40	73.9	28.6	63.8	263	79.3	132	389	9.86	2.58	5.7	27.1	63.8	261	128	0.76	0.75	0.40	11	0	15	73
		P2	75	1.1	8.20	13.4	0.39	57.9	25.6	62.9	250	48.2	125	382	6.97	1.94	16.5	24.6	62.9	249	123	0.71	0.70	0.39	15	0	10	75
	Average value		72	2.1	8.34	12.6	0.51	46.5	15.1	69.9	267	44.0	90.8	501	5.39	1.29	9.6	14.1	69.9	266	88.5	0.73	0.74	n.a.	21	0	9	70
Supraglacial meltwater	Austre Lovénbreen	AL1	13	1.3	9.10	11.2	0.04	27.4	2.3	7.8	22	28.5	16.1	36	0.53	0.16	3.0	1.8	7.8	21	14.6	0.09	0.10	0.45	12	0	39	48
Englacial meltwater		AL3	12	0.7	9.05	13.4	0.05	26.1	1.8	5.8	23	25.7	4.9	49	n.a.	0.16	3.9	1.3	5.8	23	3.5	0.09	0.08	0.13	22	0	37	41
Groundwater	Moss Land	GW	1 179	10.1	8.31	9.0	3.90	1.35×10^3	159	2.59×10^3	1.90×10^3	310	3.94×10^3	3.74×10^3	99.1	16.4	1.09×10^3	153	2.59×10^3	1.87×10^3	3.92×10^3	10.5	12.1	0.68	30	0	4	65

Note: *, data after sea-salt correction. n.a., data not available.

Table 3. Summary table for trace metal concentrations in Ny-Ålesund

Water types	Source glacier	Station	Al/ (μg·L^{-1})	Cr/ (ng·L^{-1})	Mn/ (μg·L^{-1})	Co/ (ng·L^{-1})	Cu/ (ng·L^{-1})	Fe/ (μg·L^{-1})	Zn/ (μg·L^{-1})	Cd/ (ng·L^{-1})	Pb/ (ng·L^{-1})
Ice marginal and proglacial meltwater	Austre Brøggerbreen	AB_{UP} (n = 2)	12.95	25.15	16.85	39.20	164.9	8.39	0.09	LDL	14.66
			12.10	8.59	10.77	13.86	63.47	0.61	0.11	LDL	1.25
		AB_{MD} (n = 2)	5.78	18.33	13.02	29.81	61.64	1.41	0.02	1.66	0.53
			13.00	9.21	10.48	14.64	64.09	0.69	0.00	0.53	0.94
		AB_{DW} (n = 3)	6.86	28.64	7.58	13.13	76.59	0.78	0.01	0.07	LDL
			12.52	13.12	10.15	17.20	68.24	0.27	LDL	LDL	1.08
			7.95	28.84	6.76	11.26	69.43	0.87	0.02	1.32	0.26
	Vestre Brøggerbreen	AB_{BOM} (n = 2)	14.73	54.02	1.47	11.40	103.7	7.70	0.04	0.92	7.64
			9.46	39.40	0.99	4.94	98.85	0.22	LDL	LDL	LDL
	Austre Lovénbreen	AL2	112.7	118.9	12.66	108.6	166.8	164.9	0.23	LDL	102.2
		AL4	19.28	9.98	40.42	128.6	46.27	3.43	0.12	13.02	3.41
	Pedersenbreen	P1	24.11	13.61	10.19	23.81	53.25	0.86	LDL	LDL	1.46
		P2	14.41	7.47	22.94	79.59	30.09	1.87	0.01	LDL	3.87
Average of above value			20.45	28.87	12.64	38.16	82.10	14.77	0.07	2.92	12.49
Supraglacial meltwater	Austre Lovénbreen	AL1	0.91	LDL	5.35	53.92	30.47	1.65	0.16	LDL	10.09
Englacial meltwater		AL3	3.55	3.99	6.45	25.90	17.38	4.17	0.05	0.37	3.47
Groundwater	Moss Land	GW	6.75	39.17	32.78	64.54	278.0	3.04	0.14	12.31	4.37

Note: LDL refers to the trace metal concentration is lower than the method determination limit.

166.8 ng/L, 4.96 ng/L to 128.6 ng/L, 7.47 ng/L to 118.9 ng/L, 0.26 ng/L to 102.2 ng/L, and 0.07 ng/L to 13.02 ng/L, respectively. Trace metal concentrations such as Al, Mn, Fe, Co, Zn, and Pb decreased from Site AB_{UP} to Site AB_{DW} in the Bayelva River. At the same station, larger temporal variations on different days were observed for trace metals than for major ions. For example, the coeffiecient of temporal variation (RSD) for trace metals was up to 131%, while that for major ions was no more than 40%. Except for Al and Cr, trace metal concentrations in the supraglacial and englacial meltwaters were comparable to those in the ice marginal and proglacial meltwater. For Zn, Cu, Pb and Co, higher concentrations were observed in supraglacial meltwater at AL1 than in the englacial meltwater at AL3. All metal concentrations at Site AL2 exceeded values elsewhere, with the exception of Mn. The highest Mn concentration was sampled at AL4 in Austre Lovénbreen. The lowest Mn and Co concentrations were observed in the ice marginal and proglacial meltwater from Vestre Brøggerbreen. The highest Cu concentration was found in the groundwater sample. Trace metal concentrations, except for Al, in groundwater at GW were also higher than in the nearby stream water at AB_{DW} station.

4 Discussion

4.1 *Historical hydrochemistry variations in Bayelva River*

Observations over a 20-year duration from 1990 to 2010 revealed that the retreat of the cold-based glaciers most likely led to increasing chemical weathering by longer residence time waters in the recently exposed forefield in the proglacial environment (Nowak and Hodson, 2014). Indeed, major ion concentrations, including Ca^{2+}, HCO_3^-, Mg^{2+}, SO_4^{2-}, Na^+ and K^+ nearly doubled between 2000 and 2010, caused by increased carbonate and silicate weathering (Nowak and Hodson, 2014). As shown in Fig. 2, observed carbonate weathering ion concentrations in 2015 were comparable to those in 2000 but lower than in 2010 compared to the previous study. This may reveal the annual variation of hydrochemisty in the Bayelva River during the past climate changes. However, we could not rule out that the short sampling interval during the late melt season in 2015 prevented meaningful comparisons. Alternatively, an inconsistent pattern in major ions was observed in this study compared to the historical data. For example, Na^+ and K^+ in 2015 were comparable to those in 2010, while Ca^{2+}, HCO_3^-, Mg^{2+}, SO_4^{2-}, and Si were lower. Concentrations of Na^+ and K^+ are derived from silicate weathering and are believed to have a higher Na^+ and K^+ to silicon ratio compared with the world average (Nowak and Hodson, 2014). Na^+ may be released from ion exchange by H^+ and Ca^{2+} in clay surface, while K^+ may be leached from biotite, mica and K-feldspar without the same increase of Si (Nowak and Hodson, 2014). Alternatively, similar Na^+ and K^+ concentrations compared to those in 2009 could be attributed to similar silicate weathering intensity between different expeditions, while removal of Ca^{2+} and other ions occurred. For example, a large portion of Ca^{2+} removal by absorption in high suspended sediment was observed in the outlet river of Leverett Glacier, West Greenland (Hindshaw et al., 2014). The observed inconsistent patterns reflected the variation of weathering conditions due to environmental changes in the same investigated region in different sampling period. The progressively exposed proglacial environments caused by glacial retreat would add to the variability of chemical weathering and the solute concentrations under the future climate changes, thus required continued observation.

4.2 *Weathering features revealed by meltwater hydrochemistry in Ny-Ålesund*

Solute acquisitions in meltwater come from multiple sources in the glacier basin. Following the calculation criterion defined by Hodson et al. (2000), solute provenances of sea, aerosol, crustal and atmospheric sources could be calculated by concentrations of major ions and nutrients. This provenace model ignores respired CO_2 as a contributing factor to the alkalinity budget of the water because it seems that respired CO_2 dose not significantly contribute to the water budget (Graly et al., 2017). In brief, marine provenance includes all the Cl^- and part of Ca^{2+}, Mg^{2+}, SO_4^{2-}, Na^+ and K^+ calculated from standard marine ratios to Cl^-; aerosol provenance includes all the NO_3^- and part of SO_4^{2-}; the crustal carbonate weathering and atmospheric CO_2 dominate the HCO_3^- provenance and the residual components are assumed to be derived from the crustal source. The calculated solute provenances in all ice marginal and proglacial melt-

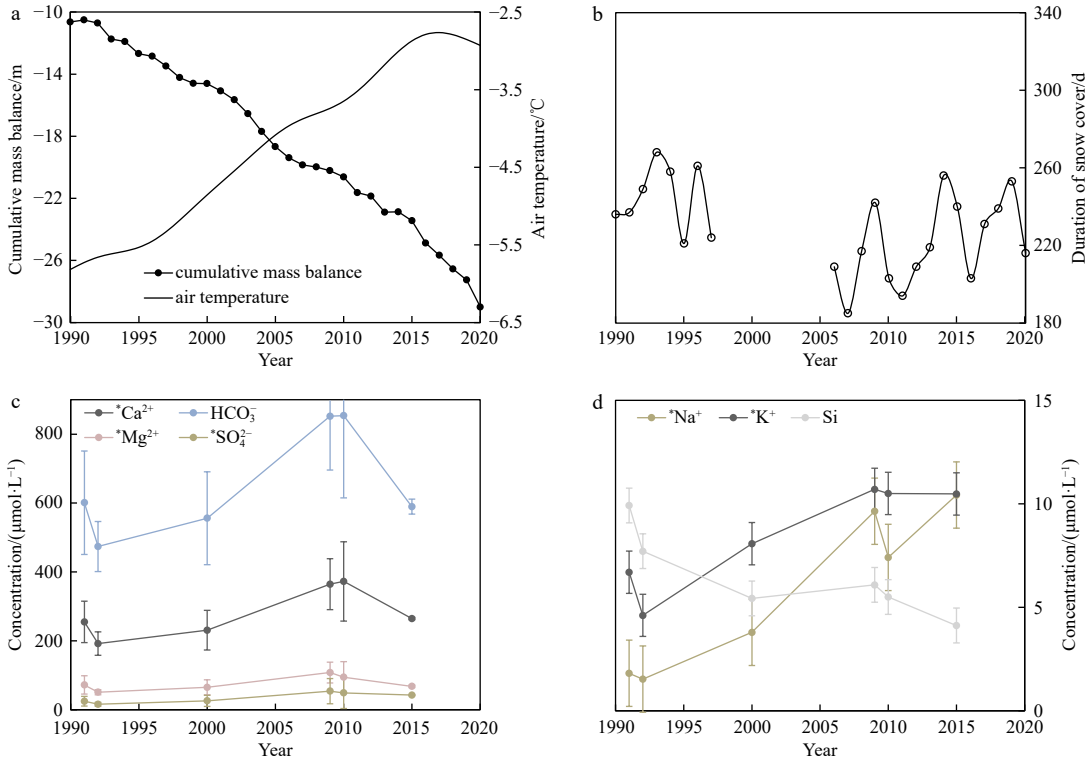

Fig. 2. Historical data of mass balance in Austre Brøggerbreen, air temperature in Ny-Ålesund, snow covered duration recorded in Svalbard Airport, and major ions in Bayelva River, during 1990–2020. Mass balance, air temperature and duration of snow cover are shown in the top panels [data source: the environmental monitoring of Svalbard and Jan Mayen Norsk (MOSJ), http://www.mosj.no/en/climate/]. Ablation seasons averaged hydrochemistry data of the Bayelva River before 2015 are obtained from Nowak and Hodson (2014), and data in 2015 are investigated in this study (the bottom panels).

water in Ny-Ålesund from atmospheric, aerosol, marine and crustal sources were 21% ± 8%, 0%, 9% ± 4%, and 70% ± 7%, respectively. For englacial and supraglacial meltwater, the crustal provenance contributed relatively lower (~40%) to the solutes, while the solutes originated from the crustal source dominated hydrochemistry in ice marginal and proglacial water of Ny-Ålesund. Besides, the Gibbs plots were used to identify the sources of major ions, including evaporative concentration, rock weathering, and atmospheric precipitation (Tranter and Wadham, 2014). Cation and anion weathering products from glacial basins confirm the dominance of rock weathering as the major source for major ions in ice marginal and proglacial meltwater in Ny-Ålesund (Fig. 3). Major ions in glacial meltwater after sea salt correction, can thus be applied to reveal the weathering features.

As shown in Fig. 4, both cation and anion ternary plots suggested a dominance of carbonate weathering in Ny-Ålesund, fol-

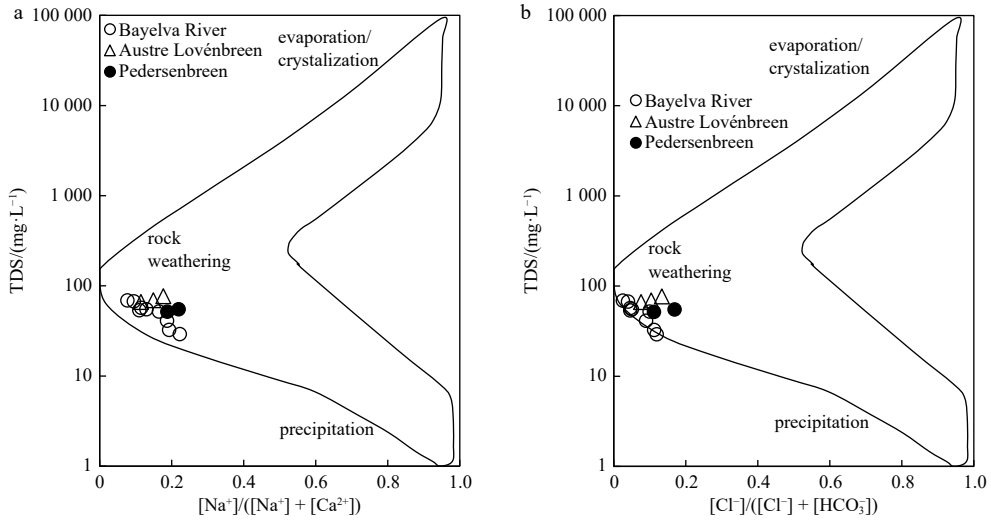

Fig. 3. Gibbs plots of total dissolved solids (TDS) versus molar ratio $[Na^+]/([Na^+] + [Ca^{2+}])$ (a), and TDS versus molar ratio $[Cl^-]/([Cl^-] + [HCO_3^-])$ (b).

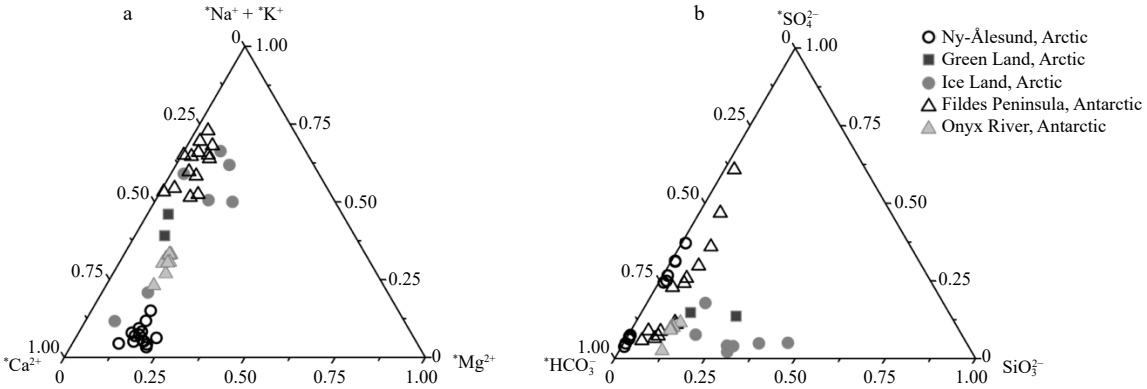

Fig. 4. Ternary plot of ions molar ratios for meltwater in Ny-Ålesund with comparison to other regions. * represents the data after sea-salt correction. Data from previous study are used for comparison (Ye et al., 2018; Jacobson et al., 2015; Yde et al., 2014; Stumpf et al., 2012; Green et al., 2005).

lowing the definition of Gaillardet et al. (1999). Ratios of [*Mg^{2+}]/[*Na^{+}] and [*Ca^{2+}]/[*Na^{+}] shown in Fig. 5a also indicated that carbonate weathering dominated the hydrology in meltwater of Ny-Ålesund, with only a small fraction of solutes coming from silicates weathering. This is consistent with previous studies based on hydrochemistry features (Nowak and Hodson, 2014; Hodson et al., 2002, 2000) and observations that bedrock types in Ny-Ålesund are mainly composed of carbonate rocks such as calcite and dolomite from Late Palaeozoic (Svendsen et al., 2002). Compared with other polar regions, such as the hydrology of Fildes Peninsula in Antarctica, Iceland and Greenland in the Arctic showed characteristics of both carbonate weathering and evaporate weathering with cations compositions. As for anion compositions, Iceland and Greenland mainly showed characteristics of silicate weathering (Figs 4 and 5a). In contrast to the weathering character in meltwaters, in groundwater sample, the ratios of [*Mg^{2+}]/[*Na^{+}] and [*Ca^{2+}]/[*Na^{+}] indicated the predominance of silicate weathering or Mg-Ca-sulphate salts dissolution (Fig. 5a). For the chemical composition of GW, the cation contained Ca^{2+} (36%), Mg^{2+} (49%), and (Na^{+}+ K^{+}) (14%) ions in μeq/L, while the anion included HCO_3^- (31%), SO_4^{2-} (66%), and Cl^- (3%) ions in μeq/L. This anions and cations composition in GW were similar to the groundwater in Finsterwalderbreen (Cooper et al., 2002), which also indicated the main weathering involved with Mg-Ca-sulphate salts dissolution and sulfide oxidation.

Though carbonate weathering dominated the hydrology in Ny-Ålesund, carbonate wearthering and silicate weathering are often coupled with other reactions, such as carbonation and sulf-

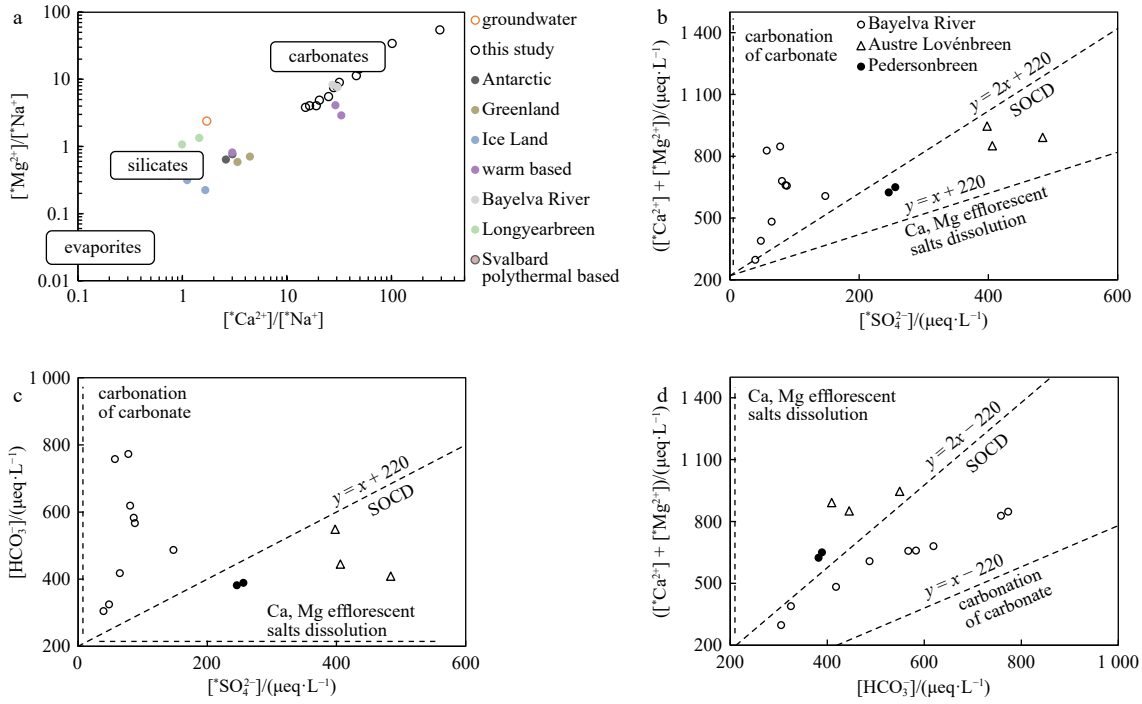

Fig. 5. Molar ratios of [*Mg^{2+}]/[*Na^{+}] versus [*Ca^{2+}]/*[Na^{+}] (a), [*Ca^{2+}] + [*Mg^{2+}] versus [*SO_4^{2-}] (b), [HCO_3^-] versus [*SO_4^{2-}] (c) and [*Ca^{2+}] + [*Mg^{2+}] versus [HCO_3^-] (d) display the compositions of glacial meltwater of Ny-Ålesund. In a, data from previous study are used for comparison (Ye et al., 2018; Jacobson et al., 2015; Nowak and Hodson, 2014; Yde et al., 2014, 2008; Feng et al., 2012; Stumpf et al., 2012; Zeng et al., 2012; Rutter et al., 2011; Green et al., 2005; Mark et al., 2005). In b–d, SOCD indicates sulfide oxidation coupled to carbonate dissolution. The dashed line represents the ion association of the corresponding weathering reaction.

ide oxidation (Stachnik et al., 2016; Nowak and Hodson, 2014). As shown in Figs 5b–d, ion ratios, slopes, and intercepts in linear regression equations from the ion association were plotted to indentify other reactions coupled with these two major weathering types, according to the definitions by Stachnik et al. (2016) and Tranter et al. (2002). Sulfate mass fraction (SMF), calculated as the ratio of $[^*SO_4^{2-}]/([^*SO_4^{2-}] + [HCO_3^-])$ in μeq/L, is used to help roughly quantify the participation of processes in weathering reactions (Stachnik et al., 2016). For example, in carbonate weathering dominated glaciers, an SMF value that equals 0.5 corresponds to the predominance of sulfide oxidation coupled with carbonate dissolution (SOCD), and an SMF below 0.5 corresponds to carbonation of carbonates dissolution (COCD), and an SMF above 0.5 is due to processes such as sulfide oxidation coupled with silicate dissolution (SOSD), carbonate precipitation, and evaporites dissolution (Cooper et al., 2002; Tranter et al., 2002). In Bayelva river and VB_{BOM} station at Vestre Brøggerbreen, ion associations were lied between the theoretical slopes of COCD and SOCD, indicating that both reactions contributed to carbonate weathering. Additionally, a small SMF value of 0.13 ± 0.04 (n = 9) revealed that the COCD was the major process. In contrast, the ion associations characrasitcs and the higher SMF value (0.45 ± 0.06, n = 5) suggested that SOCD was the dominant process in glaciers of Austre Lovénbreen and Pedersenbreen. A doubled concentration of silicate-derived solutes (Na^+, K^+ and Si) but similar total ion concentrations in meltwater of Austre Lovénbreen and Pedersenbreen were observed compared to that of AB_{DW} station in Bayelva River, suggesting a more intensive silicate weathering contribution. It is also possible that variation of SMF values could be caused by discharge; however, a long-term study in Austre Brøggerbreen showed a consistent low SMF value (<0.3) during the whole ablation season regardless of discharges (Nowak and Hodson, 2014). Therefore, the difference of SMF values between Austre Lovénbreen, Pedersenbreen, and Brøggerbreen revealed the difference of bedrock characteristics in Ny-Ålesund. Indeed, the bedrock of Brøggerbreen mainly consists of carbonate rocks of calcite and dolomite from the Late Palaeozoic (Svendsen et al., 2002). Phyllite and quartzite from Precambrian and Silurian dominate in Austre Lovénbreen and Pedersenbreen basins, with carbonate rocks from the Late Palaeozoic as minor components (Dallmann, 2015). Phyllite and quartzite are rich in silicates, corresponding to doubled silicate weathering in stream water of Austre Lovénbreen and Pedersenbreen compared to that of Bayelva River (AB_{DW} station) under the similar chemical weathering intensities. More intensed silicate weathering was firstly reported in the stream water of Austre Lovénbreen and Pedersenbreen compared to that of Bayelva River, which replenished the individual weathering difference in glaciers in Ny-Ålesund.

Finally, chemical weathering intensities (CWI) can be indicated by the sum of total crustal-derived cations (TCC) concentrations (Krawczyk et al., 2003). For all studied meltwaters, the highest CWI was observed in Austre Lovénbreen [TCC = (930 ± 39) μeq/L, n = 3], followed by Vestre Brøggerbreen [VB_{BOM} station, TCC = (853 ± 12) μeq/L, n = 2], Pedersenbreen [TCC = (674 ± 9) μeq/L, n = 2], and Austre Brøggerbreen [TCC = (554 ± 144) μeq/L, n = 7]. Solutes in meltwater runoffs may experience changes in the proglacial environment due to proglacial weathering processes and groundwater inputs. The relatively short stream length of approximately 4 km and a flowing time of about 1 h (Hodson et al., 2002) might restrict the contribution of groundwater to Bayelva River. Altnatively, chemical weathering intensity in the midstream [AB_{MD} station, (560 ± 58) μeq/L, n = 2] increased by 60% compared to the upstream [AB_{UP} station, (351 ± 48) μeq/L, n = 2] in Bayelva River, indicating solute accumulation from the active layer along the stream flow and the importance of proglacial weathering processes (Hodson et al., 2002). The CWI further increased from the midstream to the downstream [AB_{DW} station, (696 ± 10) μeq/L, n = 2] in Bayelva River may be due to the mixing with a meltwater tributary from Vestre Brøggerbreen. The high CWI [(853 ± 12) μeq/L, n = 2] in meltwater was observed at the VB_{BOM} station. If mixing caused the CWI increase at station AB_{DW}, equivalent discharge would be calculated from runoffs derived from both Austre Brøggerbreen and Vestre Brøggerbreen, which is consistant with the previous judgement by Hodson et al. (2002). For other proglacial runoffs, similar CWI along the stream flow was observed in runoffs derived from Austre Lovénbreen and Pedersenbreen, both with a short stream length of approximately 1.5 km. This implies the lack of an active layer in the bed of both short courses. However, similar SMF values and ion associations between upstream and downstream in meltwater from all investigated glaciers indicated similar weathering conditions along their meltwater flow paths. Because the groundwater sample was featured with different hydrology charateristics from silicate weathering and Mg-Ca-sulphate salts dissolution, the sample we took for groundwater may not represent a significant ion source to the proglacial runoffs in this study. Observed CWI, described by TCC concentration of (695 ± 190) μeq/L (n = 14) in Ny-Ålesund, fell at the higher end in comparison to other glacier-covered basins on Svalbard. For example, Krawczyk et al. (2003) reported that the CWI in Erikbreen, Finsterwalderbreen, Hannabreen, Midre Lovénbreen, and Scott Turnerbreen were 627 μeq/L, 600 μeq/L, 400 μeq/L, 431 μeq/L, and 308 μeq/L, respectively. Comparable CWI in cold-based glaciers, such as Vestre Brøggerbreen [VB_{BOM} station, (853 ± 12) μeq/L] and Austre Brøggerbreen upstream (AB_{DW} station, n = 2) to those found in polythermial glaciers like Erikbreen and Finsterwalderbreen demonstrate the intensive chemical weathering occuring in the recently exposed forefield by glacier retreat (Nowak and Hodson, 2014).

4.3 *Influencing factors on trace metals in meltwater from glaciers in Ny-Ålesund*

4.3.1 *Trace metals in supraglacial meltwater are mainly derived from anthropogenic deposition*

Enrichment factor (EF) value is defined as the concentration ratio of dissolved trace metals to dissolved Al in different types of meltwater, normalized to the same element ratio in the mineral soils from Bayelva area (Halbach et al., 2017). In this case, EF values of the element in meltwater are able to reveal the natural weathering or anthropogenic sources for these elements or the mobility of trace metals relative to Al in Ny-Ålesund (Dong et al., 2017; Huang et al., 2013). Overall, as shown in Fig. 6, EF values of metals in ice marginal and proglacial meltwaters were generally within range of one order of magnitude, which suggested the lithogenic sources. This is consistant with the previous knowledge that bedrock weathering is an important source for trace metals (Lehmann-Konera et al., 2021; Li et al., 2016; Aciego et al., 2015; Fortner et al., 2009; Mitchell et al., 2005). Physicochemical processes, such as absorption, desorption and precipitation, also attribute to the variations of trace metals in meltwater and have been found to affect trace metals in meltwater (Singh et al., 2017; Li et al., 2013; Fortner et al., 2009; Mitchell et al., 2006, 2005). However, in supraglacial meltwater, we found EF values of all trace metals were higher than that ranges in englacial/ice mar-

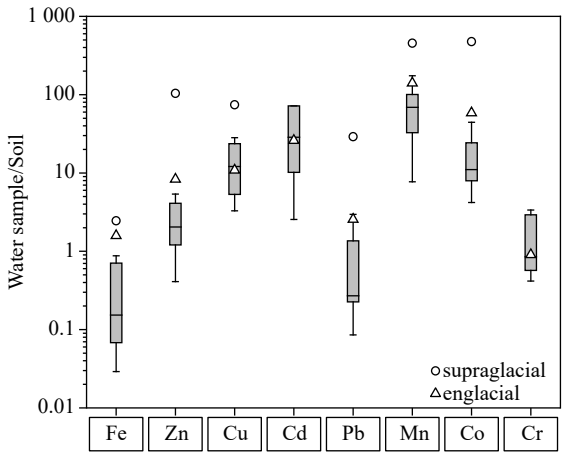

Fig. 6. Boxplot data of ratios of water concentration to soil concentration in Ny-Ålesund. All the heavy metals are normalized by Aluminum. The boxes represent the ratios of ice marginal and proglacial samples to soil, while circles and triangles represent the ratios of supraglacial and englacial water samples to soil, respectively. No supraglacial data of Cr and Cd, because they are lower than detection limit.

ginal/proglacial meltwaters, except for Cd and Cr, whose concentrations were lower than the detection limit. EF values of metals, such as Zn, Pb and Co, in supraglacial meltwater were more than 10 times higher than those in ice marginal and proglacial meltwaters, indicating an addition source. The possible source for the enrichment of metals in supraglacial meltwater is likely due to atmospheric deposition from melting snow or directly deposition, especially anthropogenic sources. Aerosols deposited in Ny-Ålesund were found from both natural and anthropogenic sources, including long-range sources mainly from Siberian local soils and reginal wildfires, and local sources mainly by fly ash emitted by cruise ships (Moroni et al., 2016). Polluted aerosols from ship emissions have been reported enriched in metals in summer, for example, Ni increased by 7 folds in aerosols emitted by cruise ships (Zhan et al., 2014). A general decreasing annual trend was reported for most observed heavy metals, except for Mn, at Zeppelin Observatory station in Ny-Ålesund over a 30-year period (Platt et al., 2022). Pb is one of the heavy metals mainly from anthropogenic sources to Ny-Ålesund (Bazzano et al., 2021), and the increasing trend of Zn was observed during the last decade (Platt et al., 2022). This is consistent with observed high EF values for Zn and Pb in supraglacial meltwaters. Thus, we conclude that trace metals in ice marginal and proglacial meltwaters are from bedrock weathering while trace metals in the supraglacial meltwater are effected by atmospheric input.

4.3.2 *Correlated trace metals in glacial meltwaters with weathering conditions*

Principal component analysis (PCA) and cluster analysis were applied to reveal metals acquisition from different processes in glacial meltwater near the ice margin. Two main components were identified from the PCA results: Principal Component 1 (PC1) and Principal Component 2 (PC2), which accounted for 32% and 25% of the total variance, respectively. As shown in Fig. 7a, based on the PCA results and the weathering properties discussed above, we identified two main groups that explain the processes controlling metal concentrations in glacial meltwater. First, we refer to Cluster 1, which is governed by carbonate weathering, resulting in significant correlation among conductivity, HCO_3^-, TDS, $*Mg^{2+}$, and $*Ca^{2+}$ ($0.72 < r < 0.97$, $p < 0.02$). Next, Cluster 2 is considered to be derived from silicate weathering, with a strong correlation among $*SO_4^{2-}$, $*K^+$, Si, and Al ($0.6 < r < 0.8$, $p < 0.01$), indicating sulfide oxidation coupled to silicate dissolution (SOSD) as an important mechanism. PCA results agreed with the obove ion association analysis. Sample sites AB_{DW} and VB_{BOM} were located in proximity to cluster 1, which is mainly characterized by carbonate weathering, while sample sites P1, P2, and AL4 were located in proximity to cluster 2, which exhibited silicate weathering signatures.

Cr was located close to cluster 1 in PCA loading plot, and was well correlated with HCO_3^- and Mg^{2+} ($0.53 < r < 0.82$, $p < 0.02$). This implied that carbonate weathering may be mainly responsible for the presence of Cr in meltwater of Ny-Ålesund. This is inconsistent with previous studies that suggested that Cr primarily originates from silicate weathering on the Tibetan Plateau (Li et al., 2016; Rudnick and Gao, 2014). Because Ny-Ålesund area was dominated by carbonate weathering with minimal silicate weathering. Also, Cr is naturally present in all rock types (Klaebe

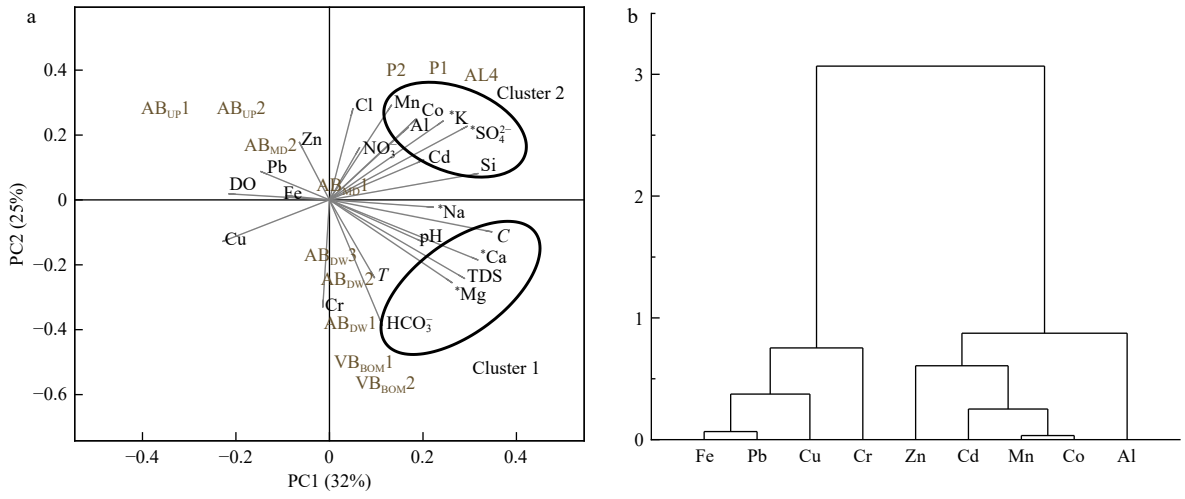

Fig. 7. a. Results of Principal Component Analysis (PCA) for chemical composition of glacial meltwater of Ny-Ålesund. Individual species are major ions, nutrients and trace elements concentrations, *C* (conductivity), *T* (temperature), pH, DO (dissolved oxygen), TDS (total dissolved solids). b. Results of cluster analysis for trace metals of glacial meltwater of Ny-Ålesund.

et al., 2021). The water-rock interaction experiments of rocks in Haut Glacier d'Arolla suggested there are no identical differences in Cr release between carbonate and silicate rocks (Mitchell et al., 2006, 2005). Cr concentration in glacial meltwater observed in Ny-Ålesund in this study is similar to Cr concentration observed in Scott River on Svalbard (Lehmann-Konera et al., 2021). Low Cr concentrations in meltwater on Svalbard compared to other region, as seen in Table 4, suggested a low baseline of Cr in local rocks on Svalbard. In this study, higher carbonate weathering was observed in Vestre Brøggerbreen and Austre Lovénbreen, as indicated by the sum of $^{*}Ca^{2+}$ and $^{*}Mg^{2+}$ of (837 ± 9.8) μeq/L and (896 ± 38.9) μeq/L, respectively, compared to Austre Brøggerbreen [(538 ± 140) μeq/L] and Pedersenbreen [(637 ± 12.9) μeq/L]. This resulted in elevated concentrations of Cr in Vestre Brøggerbreen and Austre Lovénbreen compared to Austre Brøggerbreen and Pedersenbreen.

Al, Co, Mn and Cd, were located close to cluster 2, which indicated silicate weathering origins. The presence of silicate weathering via SOSD has been identified from the major ion data, as well as previous studies in Ny-Ålesund (Nowak and Hodson, 2014). Al showed significant correlation with Si, $^{*}SO_4^{2-}$, $^{*}K^{+}$ ($0.60 < r < 0.66$, $p < 0.01$), which indicated that silicate weathering and SOSD may be responsible for Al in meltwaters. Aluminosilicate weathering is recognized as the main source of Al (Stachnik et al., 2019; Mitchell et al., 2006). Indeed, silicates in Ny-Ålesund include siliceous limestones under Brøggerbreen, and phyllite, mica-schists under Austre Lovénbreen and Pedersenbreen (Svendsen et al., 2002). Similarly, Al was found to be mainly derived from aluminosilicate weathering coupled to sulfide oxidation in Werenskiöldbreen on Svalbard (Stachnik et al., 2019). Co, Mn and Cd were found to be well correlated with $^{*}SO_4^{2-}$ ($0.75 < r < 0.86$, $p < 0.01$) and among themselves ($0.77 < r < 0.90$, $p < 0.01$) in this study (Fig. 7b). Co, Mn and Cd are usually derived from silicate weathering, e.g., quartzite, granites, gabbro, and plagioclase (Reimann and Caritat, 1998). The study supported the origin of Co, Mn, Cd from sulfide oxidation associated weathering in Ny-Ålesund. In other glacial systems, silicate weathering was also found to play an important role in the presence of Al, Co, Mn in meltwaters (Li et al., 2019). New snow is also an anthropogenic source of metals, and a positive correlation between Cl^{-} and Co, Mn were observed, implying the potential input from new snow, while correlation between Cd and Cl^{-} was not found in this study. Higher silicate weathering in Austre Lovénbreen and Pedersenbreen, as evidenced by the sum of $^{*}Na^{+}$ and $^{*}K^{+}$ of (34.4 ± 3.92) μeq/L and (36.9 ± 4.18) μeq/L, respectively, resulted in a declining trend of Al, Co, Mn, and Cd concentrations from Austre Lovénbreen and Pedersenbreen towards Austre Brøggerbreen and Vestre Brøggerbreen.

For rest of the investigated metals, Fe, Pb, Zn, and Cu, were not associated with either cluster 1 or cluster 2, and they were not correlated with major ions and other hydrochemical parameters. This implies the complexity of controlling factors in regulating these metals in Ny-Ålesund, including their various natural and anthropogenic sources (Li et al., 2019, 2016), as well as physicochemical processes in the glacier basin (Nowak and Hodson, 2015; Yde et al., 2014; Raiswell and Canfield, 2012; Wadham et al., 2010). This is also reflected by the highly spatiotemporal variations for these metals in meltwater. For example, despite similar chemical weathering intensities observed in upstream stations in Vestre Brøggerbreen and Austre Brøggerbreen, the concentrations of Fe, Zn, and Pb varied up to 35 times between two sampling expeditions. Previous studies have been found a large portion of dissolved Fe was removed along flow path in the proglacial environment in Bayelva River due to aggregation and adsorption of nanoparticulate and colloidal Fe to particles with the lack of organic complexation (Zhang et al., 2015). Intensive Fe, Zn, and Pb removal were also found in this study from the glacier output to the downstream before it entered the Kongsfjorden. Understanding of the controlling factors for trace metals in meltwater is limited in this study due to a small number of samples. We suggest a comprehensive and sustained study in this field for a better understanding of the trace metal glacial flux to the ocean under the global warming circumstances.

Concentrations of trace metals of Cr, Al, Co, Mn, and Cd exhibited regional disparities among the glaciers nearby Ny-Ålesund. There was not a clear trend of these trace metals transformation along the proglacial flow pathway. The averaged concentrations of trace metals (Al, Cr, Mn, Co, Cu, Fe, Zn, Cd, and Pb) in the ice marginal and proglacial meltwater nearby Ny-Ålesund were (20.45 ± 27.04) μg/L, (28.87 ± 29.18) ng/L, (12.64 ± 9.75) μg/L, (38.16 ± 39.11) ng/L, (82.10 ± 40.25) ng/L, (14.77 ± 43.43) μg/L, (0.07 ± 0.07) μg/L, (2.92 ± 3.41) ng/L, and (12.49 ± 28.62) ng/L, respectively. Utilizing these average trace metal concentrations and considering the glacial meltwater discharge of 0.8 km^3/a (Svendsen et al., 2002) into Kongsfjorden, we estimated the annual fluxes of Al, Cr, Mn, Co, Cu, Fe, Zn, Cd, and Pb from glacial meltwater into Kongsfjorden at approximately (16 ± 22) Mg/a, (0.02 ± 0.02) Mg/a, (10 ± 8) Mg/a, (0.03 ± 0.03) Mg/a, (0.07 ± 0.03) Mg/a, (12 ± 35) Mg/a, (0.06 ± 0.06) Mg/a, (0.002 ± 0.003) Mg/a, and (0.01 ± 0.02) Mg/a, respectively. However, the samples in this study were collected in 2015, during a period of rapid environmental changes in the Arctic. These changes are likely to alter weathering characteristics and thus the glacial meltwater flux for trace metals. Nonetheless, the data reported

Table 4. Comparison of trace metal concentration in Ny-Ålesund with other regions

Region			Al/(μg·L^{-1})	Cr/(ng·L^{-1})	Mn/(μg·L^{-1})	Co/(ng·L^{-1})	Cu/(ng·L^{-1})	Fe/(μg·L^{-1})	Zn/(μg·L^{-1})	Cd/(ng·L^{-1})	Pb/(ng·L^{-1})	Literature
Svalbard	Scott River	n = 9	1.62 ± 1.47	10 ± 11	2.58 ± 3.74	33 ± 11	54 ± 81	n.a.	0.36 ± 0.33	29 ± 22	13 ± 3	Lehmann-Konera et al. (2021)
	Ny-Ålesund	n = 13	20.5 ± 27.0	28.9 ± 29.2	12.6 ± 9.75	38.2 ± 39.1	82.1 ± 40.3	14.8 ± 43.4	0.07 ± 0.07	2.92 ± 4.55	12.5 ± 28.7	this study
Greenland	Leverett Glacier	n = 82	445	311	3.99	90.2	667	133	0.46	0.67	37.7	Hawkings et al. (2020)
	Southern Greenland	n= 16	67.5 ± 98.9	79.3 ± 96.5	6.08 ± 3.74	n.a.	541 ± 377	71.1 ± 108	1.78 ± 1.58	n.a.	n.a.	Aciego et al. (2015)
Canadian Arctic Archipelago		n = 28	5.63 ± 5.61	n.a.	1.08 ± 2.33	n.a.	308 ± 247	7.42 ± 16.1	0.11 ± 0.13	1.13 ± 0.54	2.76 ± 4.14	Colombo et al. (2019)
Switzerland	Haut Glacier d'Arolla	n = 132	35	930	9.4	100	670	390	6.7	210	200	Mitchell et al. (2006)
Antarctica	Onyx River	n = 11	n.a.	n.a.	1.26 ± 0.65	n.a.	190.6 ± 27.9	18.7 ± 16.8	0.24 ± 0.15	25.9 ± 21.5	n.a.	Green et al. (2005)

Note: n.a., data not available.

provide valuable insights for process research.

5 Conclusions

In this study, major ions and trace metals in meltwater were studied to reveal weathering and biogeochemical features in meltwaters from four glacier systems around Ny-Ålesund. The study attempts to establish a relationship between weathering and trace metals in glacial meltwaters, as well as provides a baseline study for trace metals in glacier systems in the area of Ny-Ålesund.

Major ions suggested that carbonate weathering played a dominate role in Ny-Ålesund, associated with silicate weathering and sulfide oxidation. SOCD and silicate weathering were more important in glaciers Austre Lovénbreen and Pedersenbreen. Solutes transformations reflected similar weathering conditions, and the mixing was found that corresponded to the solutes load changes.

Trace metals in supraglacial meltwater exhibited the fingerprint of anthropogenic aerosol deposition.

Principal component analysis demonstrated that Cr was correlated with carbonate weathering, while Al, Co, Mn, and Cd were correlated with silicate weathering in glacial meltwaters. Higher silicate weathering in Austre Lovénbreen and Pedersenbreen corresponded a higher content of Al, Co, Mn and Cd in glacial meltwaters. Removal of Fe, Zn, and Pb was observed from the glacier output to the downstream area before it entered Kongsfjorden, while Cr, Al, Co, Mn, and Cd exhibited regional disparities patterns. As the accelerated glacier retreat due to global warming continues, chemical components such as trace metals, which serve as trace nutrients to marine phytoplankton, derived from glaciers are subject to future changes in weathering types and intensity.

Acknowledgements

We would like to thank the Chinese Antarctic and Arctic Administration of National Oceanic Bureau and Arctic Yellow River Earth System National Observation and Research Station for the logistic support for field sampling. We are grateful to the staff at Kings Bay AS and the Chinese team members at the Yellow River Station for their assistance during our fieldwork at Ny-Ålesund, Svalbard. We also thank Prof. Seth John and Prof. James Moffett at University of Southern California for their generous offering facilities to conduct trace metals analysis. We thank Prof. Andy Hundson at University Centre in Svalbard for his valuable support to improve this manuscript.

References

Aciego S M, Stevenson E I, Arendt C A. 2015. Climate versus geological controls on glacial meltwater micronutrient production in southern Greenland. Earth and Planetary Science Letters, 424: 51–58, doi: 10.1016/j.epsl.2015.05.017

Bazzano A, Bertinetti S, Ardini F, et al. 2021. Potential source areas for atmospheric lead reaching Ny-Ålesund from 2010 to 2018. Atmosphere, 12(3): 388, doi: 10.3390/atmos12030388

Boike J, Juszak I, Lange S, et al. 2018. A 20-year record (1998–2017) of permafrost, active layer and meteorological conditions at a high Arctic permafrost research site (Bayelva, Spitsbergen). Earth System Science Data, 10(1): 355–390, doi: 10.5194/essd-10-355-2018

Colombo M, Brown K A, De Vera J, et al. 2019. Trace metal geochemistry of remote rivers in the Canadian Arctic Archipelago. Chemical Geology, 525: 479–491, doi: 10.1016/j.chemgeo.2019.08.006

Cooper R J, Wadham J L, Tranter M, et al. 2002. Groundwater hydrochemistry in the active layer of the proglacial zone, Finsterwalderbreen, Svalbard. Journal of Hydrology, 269(3–4): 208–223, doi: 10.1016/S0022-1694(02)00279-2

Dallmann W K. 2015. Geoscience Atlas of Svalbard. Tromsø: Norwegian Polar Institute Press, 133-173

Dong Z W, Qin D H, Qin X, et al. 2017. Changes in precipitating snow chemistry with seasonality in the remote Laohugou glacier basin, western Qilian Mountains. Environmental Science and Pollution Research, 24(12): 11404–11414, doi: 10.1007/s11356-017-8778-y

Feng F, Li Z Q, Jin S, et al. 2012. Hydrochemical characteristics and solute dynamics of meltwater runoff of Urumqi Glacier No. 1, eastern Tianshan, northwest China. Journal of Mountain Science, 9(4): 472–482, doi: 10.1007/s11629-012-2316-7

Fortner S K, Lyons W B, Fountain A G, et al. 2009. Trace element and major ion concentrations and dynamics in glacier snow and melt: Eliot Glacier, Oregon Cascades. Hydrological Processes, 23(21): 2987–2996, doi: 10.1002/hyp.7418

Gaillardet J, Dupré B, Louvat P, et al. 1999. Global silicate weathering and CO_2 consumption rates deduced from the chemistry of large rivers. Chemical Geology, 159(1–4): 3–30, doi: 10.1016/S0009-2541(99)00031-5

Gerringa L J A, Alderkamp A C, van Dijken G, et al. 2020. Dissolved trace metals in the Ross Sea. Frontiers in Marine Science, 7: 577098, doi: 10.3389/fmars.2020.577098

Graly J A, Drever J I, Humphrey N F. 2017. Calculating the balance between atmospheric CO_2 drawdown and organic carbon oxidation in subglacial hydrochemical systems. Global Biogeochemical Cycles, 31(4): 709–727, doi: 10.1002/2016GB005425

Graly J A, Humphrey N F, Landowski C M, et al. 2014. Chemical weathering under the greenland ice sheet. Geology, 42(6): 551–554, doi: 10.1130/G35370.1

Green W J, Stage B R, Preston A, et al. 2005. Geochemical processes in the Onyx River, Wright Valley, Antarctica: Major ions, nutrients, trace metals. Geochimica et Cosmochimica Acta, 69(4): 839–850, doi: 10.1016/j.gca.2004.08.001

Grosbois C, Négrel P, Fouillac C, et al. 2000. Dissolved load of the Loire River: Chemical and isotopic characterization. Chemical Geology, 170(1–4): 179–201, doi: 10.1016/S0009-2541(99)00247-8

Hagen J O, Kohler J, Melvold K, et al. 2003. Glaciers in Svalbard: mass balance, runoff and freshwater flux. Polar Research, 22(2): 145–159, doi: 10.3402/polar.v22i2.6452

Halbach K, Mikkelsen Ø, Berg T, et al. 2017. The presence of mercury and other trace metals in surface soils in the Norwegian Arctic. Chemosphere, 188: 567–574, doi: 10.1016/j.chemosphere.2017.09.012

Haldorsen S, Heim M, Van Der Ploeg M. 2011. Impacts of climate change on groundwater in permafrost areas: Case study from Svalbard, Norway. In: Treidel H, Martin-Bordes J L, Gurdak J J, eds. Climate Change Effects on Groundwater Resources. London: CRC Press, 341–356, doi: 10.1201/b11611-26

Hawkings J R, Skidmore M L, Wadham J L, et al. 2020. Enhanced trace element mobilization by Earth's ice sheets. Proceedings of the National Academy of Sciences of the United States of America, 117(50): 31648–31659, doi: 10.1073/pnas.2014378117

Hindshaw R S, Rickli J, Leuthold J, et al. 2014. Identifying weathering sources and processes in an outlet glacier of the Greenland Ice Sheet using Ca and Sr isotope ratios. Geochimica et Cosmochimica Acta, 145: 50–71, doi: 10.1016/j.gca.2014.09.016

Hodson A, Tranter M, Gurnell A, et al. 2002. The hydrochemistry of Bayelva, a high Arctic proglacial stream in Svalbard. Journal of Hydrology, 257(1–4): 91–114, doi: 10.1016/S0022-1694(01)00543-1

Hodson A, Tranter M, Vatne G. 2000. Contemporary rates of chemical denudation and atmospheric CO_2 sequestration in glacier basins: An Arctic perspective. Earth Surface Processes and Landforms, 25(13): 1447–1471, doi: 10.1002/1096-9837(200012)25:13<1447::AID-ESP156>3.0.CO;2-9

Hop H, Falk-Petersen S, Svendsen H, et al. 2006. Physical and biological characteristics of the pelagic system across Fram Strait to Kongsfjorden. Progress in Oceanography, 71(2–4): 182–231, doi: 10.1016/j.pocean.2006.09.007

Huang J, Kang S C, Zhang Q G, et al. 2013. Atmospheric deposition of trace elements recorded in snow from the Mt. Nyainqêntanglha region, southern Tibetan Plateau. Chemosphere, 92(8): 871–881, doi: 10.1016/j.chemosphere.2013.02.038

Huertas M J, López-Maury L, Giner-Lamia J, et al. 2014. Metals in cyanobacteria: Analysis of the copper, nickel, cobalt and arsenic homeostasis mechanisms. Life, 4(4): 865–886, doi: 10.3390/life4040865

Hugonnet R, McNabb R, Berthier E, et al. 2021. Accelerated global glacier mass loss in the early twenty-first century. Nature, 592(7856): 726–731, doi: 10.1038/s41586-021-03436-z

Ingri J, Widerlund A, Land M. 2005. Geochemistry of major elements in a pristine boreal river system; hydrological compartments and flow paths. Aquatic Geochemistry, 11(1): 57–88, doi: 10.1007/s10498-004-2248-0

IPCC. 2019. IPCC Special Report on the Ocean and Cryosphere in A Changing Climate (Pörtner H O, Roberts D C, Masson-Delmotte V, et al. , eds.). Cambridge and New York: Cambridge University Press

Irvine-Fynn T D L, Bridge J W, Hodson A J. 2010. Rapid quantification of cryoconite: Granule geometry and in situ supraglacial extents, using examples from Svalbard and Greenland. Journal of Glaciology, 56(196): 297–308, doi: 10.3189/002214310791968421

Irvine-Fynn T D L, Hodson A J. 2010. Biogeochemistry and dissolved oxygen dynamics at a subglacial upwelling, Midtre Lovénbreen, Svalbard. Annals of Glaciology, 51(56): 41–46, doi: 10.3189/172756411795931903

Jacobson A D, Grace Andrews M, Lehn G O, et al. 2015. Silicate versus carbonate weathering in Iceland: New insights from Ca isotopes. Earth and Planetary Science Letters, 416: 132–142, doi: 10.1016/j.epsl.2015.01.030

Klaebe R, Swart P, Frei R. 2021. Chromium isotope heterogeneity on a modern carbonate platform. Chemical Geology, 573: 120227, doi: 10.1016/j.chemgeo.2021.120227

Krawczyk W E, Lefauconnier B, Pettersson L E. 2003. Chemical denudation rates in the Bayelva Catchment, Svalbard, in the Fall of 2000. Physics and Chemistry of the Earth, Parts A/B/C, 28(28–32): 1257–1271, doi: 10.1016/j.pce.2003.08.054

Lehmann-Konera S, Kociuba W, Chmiel S, et al. 2021. Effects of biotransport and hydro-meteorological conditions on transport of trace elements in the Scott River (Bellsund, Spitsbergen). PeerJ, 9: e11477, doi: 10.7717/peerj.11477

Li X Y, Ding Y J, Hood E, et al. 2019. Dissolved iron supply from Asian Glaciers: Local controls and a regional perspective. Global Biogeochemical Cycles, 33(10): 1223–1237, doi: 10.1029/2018GB006113

Li X Y, He X B, Kang S C, et al. 2016. Diurnal dynamics of minor and trace elements in stream water draining Dongkemadi Glacier on the Tibetan Plateau and its environmental implications. Journal of Hydrology, 541: 1104–1118, doi: 10.1016/j.jhydrol.2016.08.021

Li X Y, Qin D H, Jing Z F, et al. 2013. Diurnal hydrological controls and non-filtration effects on minor and trace elements in stream water draining the Qiyi Glacier, Qilian Mountain. Science China Earth Sciences, 56(1): 81–92, doi: 10.1007/s11430-012-4480-6

Mark B G, McKenzie J M, Gómez J. 2005. Hydrochemical evaluation of changing glacier meltwater contribution to stream discharge: Callejon de Huaylas, Peru. Hydrological Sciences Journal, 50(6): 975–987, doi: 10.1623/hysj.2005.50.6.975

Miao A J, Wang W X, Juneau P. 2005. Comparison of Cd, Cu, and Zn toxic effects on four marine phytoplankton by pulse-amplitude-modulated fluorometry. Environmental Toxicology and Chemistry, 24(10): 2603–2611, doi: 10.1897/05-009R.1

Millero F J, Graham T B, Huang F, et al. 2006. Dissociation constants of carbonic acid in seawater as a function of salinity and temperature. Marine Chemistry, 100(1–2): 80–94, doi: 10.1016/j.marchem.2005.12.001

Mitchell A C, Brown G H, Fuge R. 2005. Are minor and trace elements useful indicators of chemical weathering processes and flow-routing in subglacial hydrological systems?. In: Robert H, Susan F, eds. 62nd Eastern Snow Conference. Ontario: Waterloo Press , 49–67

Mitchell A C, Brown G H, Fuge R. 2006. Minor and trace elements as indicators of solute provenance and flow routing in a subglacial hydrological system. Hydrological Processes, 20(4): 877–897, doi: 10.1002/hyp.6112

Morel F M M, Price N M. 2003. The biogeochemical cycles of trace metals in the oceans. Science, 300(5621): 944–947, doi: 10.1126/science.1083545

Moroni B, Cappelletti D, Ferrero L, et al. 2016. Local vs. long-range sources of aerosol particles upon Ny-Ålesund (Svalbard Islands): mineral chemistry and geochemical records. Rendiconti Lincei, 27(1): 115–127, doi: 10.1007/s12210-016-0533-7

Nowak A, Hodson A. 2013. Hydrological response of a High-Arctic catchment to changing climate over the past 35 years: A case study of Bayelva watershed, Svalbard. Polar Research, 32(1): 19691, doi: 10.3402/polar.v32i0.19691

Nowak A, Hodson A. 2014. Changes in meltwater chemistry over a 20-year period following a thermal regime switch from polythermal to cold-based glaciation at Austre Brøggerbreen, Svalbard. Polar Research, 33(1): 22779, doi: 10.3402/polar.v33.22779

Nowak A, Hodson A. 2015. On the biogeochemical response of a glacierized High Arctic watershed to climate change: Revealing patterns, processes and heterogeneity among micro-catchments. Hydrological Processes, 29(6): 1588–1603, doi: 10.1002/hyp.10263

Perlt E, von Domaros M, Kirchner B, et al. 2017. Predicting the ionic product of water. Scientific Reports, 7: 10244, doi: 10.1038/s41598-017-10156-w

Platt S M, Hov Ø, Berg T, et al. 2022. Atmospheric composition in the European Arctic and 30 years of the Zeppelin Observatory, Ny-Ålesund. Atmospheric Chemistry and Physics, 22(5): 3321–3369, doi: 10.5194/acp-22-3321-2022

Pratush A, Kumar A, Hu Z. 2018. Adverse effect of heavy metals (As, Pb, Hg, and Cr) on health and their bioremediation strategies: a review. International Microbiology, 21(3): 97–106, doi: 10.1007/s10123-018-0012-3

Raiswell R, Canfield D E. 2012. The iron biogeochemical cycle past and present. Geochemical Perspectives, 1(1): 1–220, doi: 10.7185/geochempersp.1.1

Rajaram R, Ganeshkumar A, Emmanuel Charles P. 2023. Ecological risk assessment of metals in the Arctic environment with emphasis on Kongsfjorden Fjord and freshwater lakes of Ny-Ålesund, Svalbard. Chemosphere, 310: 136737, doi: 10.1016/j.chemosphere.2022.136737

Reimann C, Caritat P. 1998. Chemical Elements in the Environment. Berlin, Heidelberg: Springer, Berlin, Heidelberg, doi: 10.1007/978-3-642-72016-1

Ren J L, Zhang J, Li J B, et al. 2006. Dissolved aluminum in the Yellow Sea and East China Sea - Al as a tracer of Changjiang (Yangtze River) discharge and Kuroshio incursion. Estuarine, Coastal and Shelf Science, 68(1–2): 165–174, doi: 10.1016/j.ecss.2006.02.004

Rudnick R L, Gao S. 2014. Composition of the continental crust. In: Rudnick R L, ed. Treatise on Geochemistry. 2nd ed. Amsterdam: Elsevier, 4: 1–51, doi: 10.1016/B978-0-08-095975-7.00301-6

Rutter N, Hodson A, Irvine-Fynn T, et al. 2011. Hydrology and hydrochemistry of a deglaciating high-Arctic catchment, Svalbard. Journal of Hydrology, 410(1–2): 39–50, doi: 10.1016/j.jhydrol.2011.09.001

Singh A T, Laluraj C M, Sharma P, et al. 2017. Export fluxes of geochemical solutes in the meltwater stream of Sutri Dhaka Glacier, Chandra basin, Western Himalaya. Environmental Monitoring and Assessment, 189(11): 555, doi: 10.1007/s10661-017-6268-9

Stachnik Ł, Majchrowska E, Yde J C, et al. 2016. Chemical denudation and the role of sulfide oxidation at Werenskioldbreen, Svalbard. Journal of Hydrology, 538: 177–193, doi: 10.1016/j.jhydrol.2016.03.059

Stachnik Ł, Yde J C, Nawrot A, et al. 2019. Aluminium in glacial meltwater demonstrates an association with nutrient export (Werenskiöldbreen, Svalbard). Hydrological Processes, 33(12): 1638–1657, doi: 10.1002/hyp.13426

Stumpf A R, Elwood Madden M E, Soreghan G S, et al. 2012. Glacier meltwater stream chemistry in Wright and Taylor Valleys, Antarctica: Significant roles of drift, dust and biological processes in chemical weathering in a polar climate. Chemical Geology, 322–323: 79–90, doi: 10.1016/j.chemgeo.2012.06.009

Svendsen H, Beszczynska-Møller A, Hagen J O, et al. 2002. The physical environment of Kongsfjorden – Krossfjorden, an Arctic fjord system in Svalbard. Polar Research, 21(1): 133–166, doi: 10.1111/j.1751-8369.2002.tb00072.x

Tagliabue A, Bowie A R, Boyd P W, et al. 2017. The integral role of iron in ocean biogeochemistry. Nature, 543(7643): 51–59, doi: 10.1038/nature21058

Tranter M, Sharp M J, Lamb H R, et al. 2002. Geochemical weathering at the bed of Haut glacier d'Arolla, Switzerland - A new model. Hydrological Processes, 16(5): 959–993, doi: 10.1002/hyp.309

Tranter M, Wadham J L. 2014. Geochemical weathering in glacial and proglacial environments. In: Holland H D, Turekian K K, eds. Treatise on Geochemistry. 2nd ed. Amsterdam: Elsevier, 7: 157–173

Vance D, Little S H, De Souza G F, et al. 2017. Silicon and zinc biogeochemical cycles coupled through the Southern Ocean. Nature Geoscience, 10(3): 202–206, doi: 10.1038/ngeo2890

Vargo L J, Anderson B M, Dadić R, et al. 2020. Anthropogenic warming forces extreme annual glacier mass loss. Nature Climate Change, 10(9): 856–861, doi: 10.1038/s41558-020-0849-2

Wadham J L, Tranter M, Hodson A J, et al. 2010. Hydro-biogeochemical coupling beneath a large polythermal Arctic glacier: Implications for subice sheet biogeochemistry. Journal of Geophysical Research: Earth Surface, 115(F4): F04017, doi: 10.1029/2009JF001602

Willis K, Cottier F, Kwasniewski S, et al. 2006. The influence of advection on zooplankton community composition in an Arctic fjord (Kongsfjorden, Svalbard). Journal of Marine Systems, 61(1–2): 39–54, doi: 10.1016/j.jmarsys.2005.11.013

Woosley R J, Moon J Y. 2023. Re-evaluation of carbonic acid dissociation constants across conditions and the implications for ocean acidification. Marine Chemistry, 250: 104247, doi: 10.1016/j.marchem.2023.104247

Yde J C, Knudsen N T, Hasholt B, et al. 2014. Meltwater chemistry and solute export from a Greenland Ice Sheet catchment, Watson River, West Greenland. Journal of Hydrology, 519: 2165–2179, doi: 10.1016/j.jhydrol.2014.10.018

Yde J C, Riger-Kusk M, Christiansen H H, et al. 2008. Hydrochemical characteristics of bulk meltwater from an entire ablation season, Longyearbreen, Svalbard. Journal of Glaciology, 54(185): 259–272, doi: 10.3189/002214308784886234

Ye L P, Zhang R F, Sun Q Z, et al. 2018. Hydrochemistry of the meltwater streams on Fildes Peninsula, King George Island, Antarctica. Journal of Oceanology and Limnology, 36(6): 2181–2193, doi: 10.1007/s00343-019-7193-2

Zeng C, Gremaud V, Zeng H T, et al. 2012. Temperature-driven meltwater production and hydrochemical variations at a glaciated alpine karst aquifer: Implication for the atmospheric CO_2 sink under global warming. Environmental Earth Sciences, 65(8): 2285–2297, doi: 10.1007/s12665-011-1160-3

Zhan J Q, Gao Y, Li W, et al. 2014. Effects of ship emissions on summertime aerosols at Ny-Alesund in the Arctic. Atmospheric Pollution Research, 5(3): 500–510, doi: 10.5094/APR.2014.059

Zhang R F, John S G, Zhang J, et al. 2015. Transport and reaction of iron and iron stable isotopes in glacial meltwaters on Svalbard near Kongsfjorden: From rivers to estuary to ocean. Earth and Planetary Science Letters, 424: 201–211, doi: 10.1016/j.epsl.2015.05.031